EEG based Absence Epilepsy detection

Bárbara Bica [1], Jorge Figueroa [2], Lisa Salgueiro [3], Rojan Aslani [4], Joaquim Alves [✉]
(1)1190415@isep.ipp.pt,
(2)1210359@isep.ipp.pt,
(3)1190810@isep.ipp.pt,
(4)1191398@isep.ipp.pt,
(✉)jaa@isep.ipp.pt
Instituto Superior de Engenharia do Porto, Porto, Portugal

Abstract— Childhood Absence Epilepsy (CAE) is a type of epilepsy, a well-known condition that is characterized by seizures, which derivate from an abnormal brain electrical activity. This disease is more incident in children and manifests through a loss of consciousness of the present moment, being often interpreted as daydreaming. With the great advances in recording electroencephalogram (EEG) signals, it has become possible to analyze these signals in an automated manner for information extraction to help in seizure detection and prediction. Due to the brevity and subtle manifestations, absence seizures can be easily missed by inexperienced observers, and they are challenging to detect even for experienced medical staff. In this project we applied signal processing to detect CAE epileptic activity in EEG signals.
In this work, an algorithm was implemented to determine whether a patient has signs of CAE with resort to an EEG sample. To do so, a preprocessing of the signal was done to remove unwanted components. The method used for detecting the spike waves is cross correlation. Nine different samples of spike wave segments were extracted from different EEG signals (with diagnosis of CAE), and the EEG signal under study is correlated with all 9 of the selected spike waves.
EEG samples from 5 patients with different severity of CAE diagnosis were used to test the accuracy of the implemented algorithm. All cases with CAE were detected. A control EEG sample was used to test for false positives. In this file no discharge was detected. The execution time for the whole algorithm (including the uploading of the EEG signal, processing, and finalizing) take about 250 seconds on an Intel Core i5 CPU computer.
In future works a larger database should be used to evaluate the functionality of this algorithm. Ideally, the execution time should be decreased, and real-time application of the algorithm to EEG signal should be tested.

Keywords—absence epilepsy, EEG signal decomposition, spike detection algorithm, EEG correlation analysis.

1 Introduction

1.1 Electroencephalography

Scalp electroencephalography (EEG), a noninvasive medical imaging technique, is defined as an electrical activity recorded from the surface of the scalp with the help of metal electrodes and a conducting medium (Figure 1). It is an easily available test that provides evidence of how the brain functions over time. For clinical neurophysiology and neurology, EEG has been found to be very useful. A local current is generated when neurons in the brain are activated during synaptic excitations of the dendrites and is measured as EEG (Niedermeyer & Lopes da Silva, 1993; Siuly, Li, & Zhang, 2016).
Electroencephalographic reading is a completely safe procedure that can be conducted repeatedly on patients, normal adults, and children without any risk or limitation. The local current flow is caused by active neurons consisting of different ions that are expelled through channels in neuron membranes in the direction governed by membrane potential (HL & WA, 1989). The recordable electrical activity is created on the head surface. Between electrode and neuronal layers, the current penetrates through skin, skull, and

several other layers (See details see AAppendix I. Generation of electrical fields in brain.). The signals detected through electrodes are weak, so they are amplified, digitized, and stored to computer memory (FS & JR, 1989).

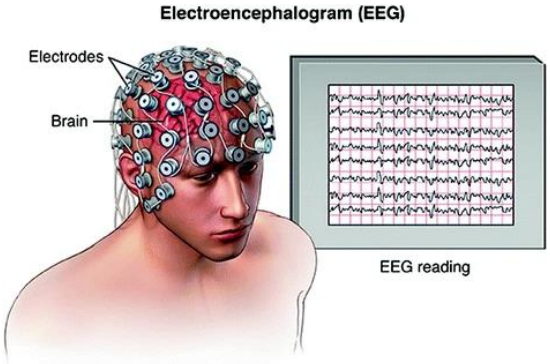

Figure 1. An illustration of EEG recording (Ref. (Siuly, Li, & Zhang, 2016)).

1.2 Brain waves

Brain waves are oscillating electrical voltages in the brain measuring just a few millionths of a volt. There are five widely recognized human brain waves which are presented in Figure 2 along with their frequencies, some characteristics, and waveforms (Abhang, Gawali, & Mehrotra, 2016). It is important to mention that gamma waves are fast oscillations with small amplitude and high contamination by muscle artifacts, making these waves underestimated and not widely studied as compared to other slow brain waves (Malik & Ullah Amin, 2017).

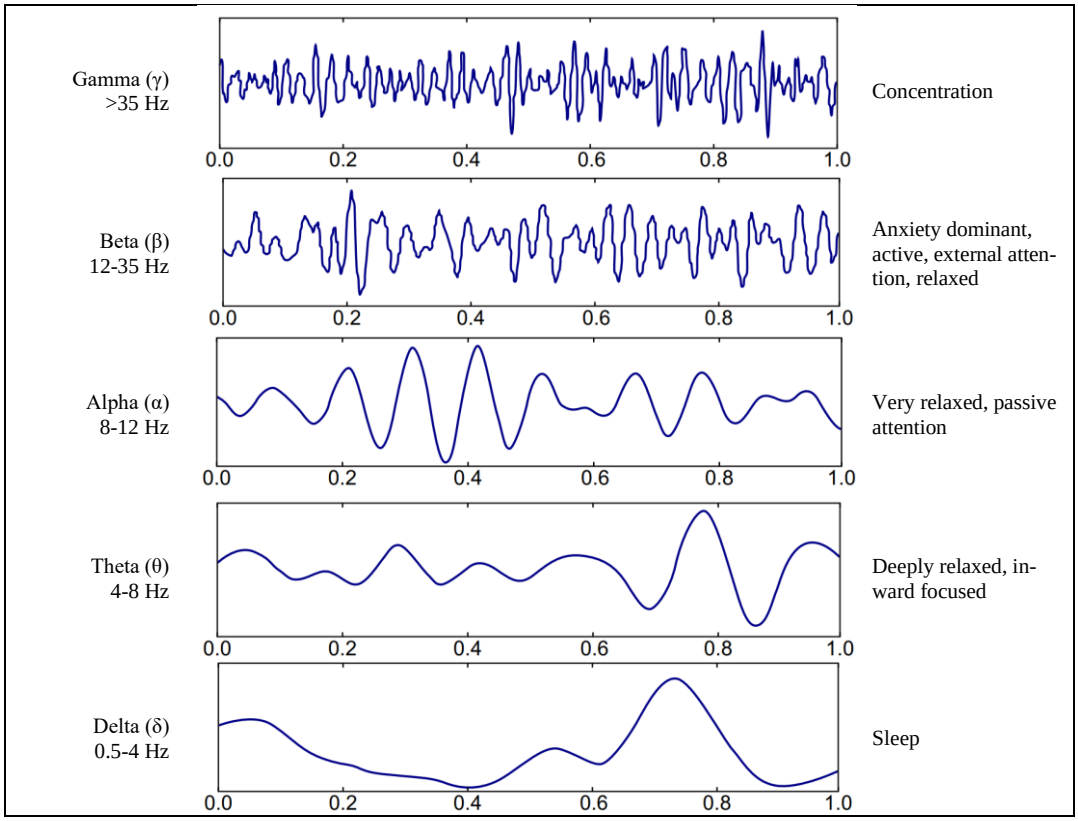

Figure 2. Characteristics of 5 basic brain waves of healthy adults (ref. (Abhang, Gawali, & Mehrotra, 2016)).

1.3 Childhood Absence Epilepsy

Epilepsy is a neurological condition that causes seizures due to bursts of abnormal brain electrical activity. Epilepsy is not an age-related disease and can be manifested in different types of seizures (NHS, n.d.). Generalized seizures affect both the left and right sides of the brain and can be classified into motor or non-motor. A motor seizure can be accompanied by muscle twitching, jerking movements, weakness, and full-body spasms, among others. On the other hand, non-motor seizures or absence seizures can be manifested through brief twitches, staring into space or fluttering eyelids (Medical News Today, n.d.).

Absence Epilepsy, (also known as Childhood Absent Epilepsy (CAE)) is characterized by unusual brain electrical activity found in both hemispheres of the brain, with the seizures being accompanied with a loss of consciousness. As the name indicates, this condition is mostly diagnosed in children, with an incidence of 2 to 8 in 100,000 in children up to 16 years old (Jon-Paul A. Manning, 2003). These types of seizures are often set off by a period of hyperventilation (Johns Hopkins Medicine, n.d.).

In CAE, seizures are frequent and brief, lasting just a few seconds. Some children can have many seizures per day. In other epilepsies, particularly those with an older age of onset, the seizures can last several seconds to minutes and may occur only a few times a day (Dan, Vandendriessche, Paesschen, Weckhuysen, & Bertrand, 2020).

Absence seizures can be classified depending on the clinical characteristics and electroencephalography as: Typical Absence, Atypical Absence, Myoclonic Absence, and Eyelid Myoclonia. The generalized idiopathic epilepsies also have age-related onset. CAE onset is at age 4-8 years, with peak onset at age 6-7 years. Juvenile Absence Epilepsy onset is generally around puberty, mostly between 10-19 years, with a peak at 15 years (Albuja & Khan., 2021).

There is a positive family history of epilepsy in 15% to 44% in CAE, and particularly in parents and siblings, the frequency for each is between 42.6% and 20.7%, respectively. Even though it is genetically determined, the inheritance and genes involved remain unidentified (Sara Matricardi MD, 2014).

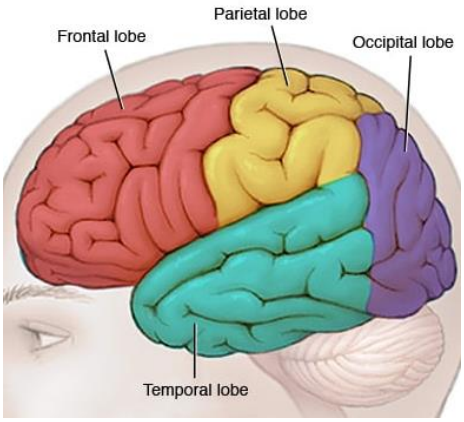

Figure 3. Sagittal view of the human brain *(Frontiers, s.f.)*.

The CAE relates to a suspension of the working memory (a frontal lobe function), which explains the immediate restoration of the impaired neurocognitive functions right at the termination of the seizures (A. Pavone, 2000). Studies show that the evolution of CAE forms a big part in the frontal lobe, as beginning with “discrete, often unilateral spikes in the frontal regions and evolve to engage frontal and mesial frontal (or middle) regions as well as the temporal lobes during the repeating spike and wave cycles” (Rochelle Caplan) (See Figure *3*). The involvement of the orbital and inferior frontal, and dorsolateral

prefrontal gyrus in behavior, cognition and language suggest that structural abnormalities might be related to the difficulties in with CAE.

The main diagnostic tool for absence seizures detection is the EEG. Ictal discharges are the discharges manifested during a seizure, whereas interictal discharges occur between seizures (Robert S. Fisher, 2015). Characteristic ictal and interictal discharges can be found.

In the case of a typical CAE, the EEG shows bilaterally synchronous and symmetrical 3-Hertz (Hz) spike-and-wave discharges (SWD) that start and end abruptly, maximal over frontal regions (Figure *3*). These SWD complexes coincide with the abrupt onset and offset of the ictal phenomena. Short interictal discharges may not be associated with considerable clinical manifestations but sequences of SWD complexes that last more than a few seconds are generally associated with Typical Absence seizures (M.D., 2006). Atypical Absence seizures show a more insidious onset and offset, less symmetrical and slower spike-and-wave seizures (less than 3 Hz: 1.5 to 2.5 Hz), and an abnormal interictal background (M.D., 2006).

Since the SWD patterns characteristic of absence seizures have a frequency of 3 Hz, the delta band (0.5 – 4 Hz) is the frequency band of interest (Xanthopoulos, Rebennack, Liu, & Zhang, 2010).

Spikes are the primary form of discharge in CAE (20-70 ms as their time length). After this type, the spike-slow wave appears (200-500 ms as their time length). The sharp waves also appear, which can be very similar to the primary from but differ in their length (70-200 ms) as their time length). (Taeho Kim, 2020) The difference between these different types of waves is their duration (see Figure 4). These waves are interictal discharges.

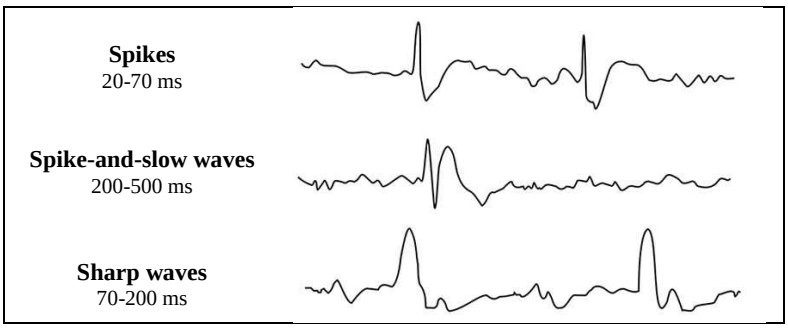

Figure 4. Graphic representation of different SWDs (Taeho Kim, 2020).

Taking into consideration that seizures are different from person to person, and the only known parameters that could maintain in a fixed value are the duration and the shape of the waves, it can be stated that the general frequency of each wave is hard to find. Currently the method used by health professionals and to detect epileptic discharge is by visual assessment of the EEG.

2 State of the art

A summary of the reviewed state of the art about CAE detection algorithms is presented in Table 1.

Table 1. Summary of the state of the art.

Filter type	Order	Cutoff frequency (Hz)	Motive	Ref.
IIP	2	50	Remove power line noise	(Glaba, Latka, & West, 2021)
High-pass Butterworth	6	0.5	Remove EEG baseline drift	
Low-pass Butterworth	6	25	Remove muscle artifacts	
High-pass Butterworth	4	0.5	-	(Dan, Vandendriessche, Paesschen, Weckhuysen, & Bertrand, 2020)
Low-pass Butterworth	4	25	-	
Down-sampling	-	-	-	
Finite Impulse Response	-	-	-	
Low pass filter	-	30	Decrease high frequency noise embedded in recordings	(Xanthopoulos, Rebennack, Liu, & Zhang, 2010)
Wavelet decomposition	-	-	-	
Sliding variance technique	-	-	-	
Thresholds application	-	-	-	
band pass	-	0.53–25 Hz	-	(Nadia Mammone, 2015)
Sliding temporal window			-	
Low pass	-	25	-	(Berman, Negishi, Vestal, & Spann, 2010)
Built in low-pass Butterworth filter	-	-	-	
Adaptive noise cancellation software	-	-	-	
High pass	-	0.5	-	(Hao, Khoo, Ellenrieder, Zazubovits, & Gotman, 2018)
Low pass	-	50	-	
Band pass	-	0.1 – 44	-	(Tuncera & Bolat, 2022)
Band pass	-	0.5 – 150	-	
High pass	-	-	Low frequency components are eliminated, and the detail component is obtained.	
Low pass	-	-	Analysis of low frequency components	
Wavelet (DWT) Range 0-31	-	25	-	

3 Data information

3.1 Subjects

The EEG samples from patients with CAE were kindly offered by Neuroimprove clinic (www.neuroimprove.pt). Details about the samples are presented in Table 2. None of the patients are consuming regular medication.

Table 2. Subject data.

Sample name	Pathology	Age	Gender	Acquisition date
1642C_Moderate	Epilepsy	16	Male	20/04/2022
1316C_Moderate	Moderate epilepsy	4	Male	08/11/2021
1564C_Sever	Severe epilepsy	6	Female	16/05/2022
1573C_Benign	Benign epilepsy	6	Male	09/03/2022
1638C_Control	None	7	Male	19/04/2022

3.2 EEG acquisition

The EEG acquisition was done with BrainMaster Discovery Hardware using the NeuroGuide 3.1.0 software. The EEG data was acquired using 22 gold-plated electrodes (19 channels, 2 reference and 1 ground electrodes), positioned according to the international 10-20 system, which can be consulted in Appendix II. 10-20 electrode positioning system.. The sampling frequency of all EEG signals is 256 Hz. For each subject, a trained expert reviewed the EEG recordings and identified the habitual epileptic discharges (Aslani, 2022).

4 EEG signal processing

The signal processing of the EEG signal was conducted in GNU Octave (version 7.1.0) resorting to the open-source packages, namely *io* and *signal* packages. The *io* package was used to manipulate Excel file. *Signal* package was used to access functions such as *fft(), ifft(),* and *xcorr()*.
To detect the epileptic activity in the EEG signal, filtering and processing was performed before applying the spike detection algorithms. The processes were chosen based on the state of the art, but further testing was done to choose the most adequate one for this application. The high-level block diagram is presented in Figure 5.

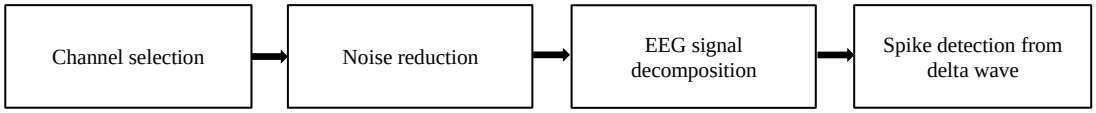

Figure 5. High-level block diagram of processing of EEG signal to detect epileptic activity.

A. EEG Channel selection

Knowing that the mesial portion of the frontal lobes are the regions of the brain most affected by epileptic activity, the electrodes positioned in the center of these structures was chosen for processing. Knowing that the EEG signal was acquired by 10-20 system (Appendix II. 10-20 electrode positioning system.), and according to the naming of the columns in the EEG text file, it was determined that Fz channel (7^{th} channel) was chosen in the next steps of the algorithm.

A. Noise reduction

To facilitate and enable the detection of epileptic activity, it is necessary to reduce the noise components such as the power line noise, baseline drift, muscle activity artefacts, etc. As mentioned before, the gamma wave is barely studied, and is considered irrelevant to our study, hence, the frequency range of this wave can be removed from the signal at this stage.
By limiting the maximum frequency to 35 Hz, many noise components are removed, considering that the powerline noise is 50 or 60 Hz (depending on the country where the signal was acquired), as well as some of the muscle activity artefacts. The minimum cut-off frequency was set to 0.5 not only because the delta wave lies between the interval of 0.5 to 4 Hz, but also to cut out the DC components of the EEG signal.
It is relevant to mention that the data used in this project already has the power line noise removed. Nevertheless, our algorithm filters this noise so that it is applicable to other EEG signals, the block diagram of which is presented in Figure 6.

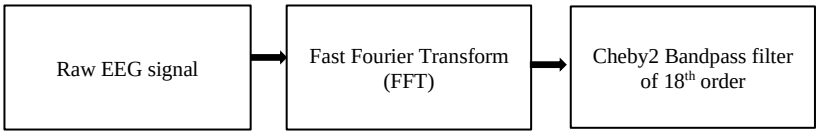

Figure 6. Block diagram of noise removal algorithm.

1) Exploiting the frequency domain

The Fast Fourier Transform (FFT) is an optimized algorithm for the implementation of the Discrete Fourier Transformation. A signal is sampled over a period and divided into

its frequency components. These components are single sinusoidal oscillations at distinct frequencies each with their own amplitude and phase (NTI Audio, 2022). In this project, FFT was applied to the EEG signal, as it enables the analysis and processing the frequencies present in the signal. The length of FFT is based on each EEG signal, being equal to the next power of two in comparison to the length of the EEG. With the FFT being longer than the EEG signal, this procedure automatically fills in the remaining samples with zeros. The extra zeros created were removed in next steps.

2) Chebyshev type II bandpass filter

To limit the frequencies of the signal to the desired ones, a Chebyshev type II bandpass filter of 18^{th} order was applied. This filter was chosen because it provides a steeper transition phase than the Butterworth, Chebyshev type I, and elliptic filter, as well as having lower ripple. The cutoff frequencies (higher cutoff frequency (fc-high) 35 Hz, and lower cutoff frequency (fc-low) 0.5 Hz) were chosen according to earlier explanation. Type II Chebyshev filter has no ripple in the passband because of the high roll off rate (rate of change of the output of the filter versus frequency), which is a remarkable characteristic of the Chebyshev filter. The bigger the order of the filter, the bigger is the roll off.
In the case of this study, the next step of the algorithm will remove these components from the signal, so this step was practically unnecessary. Nonetheless, it was applied to the signal, in case of future alterations in the spike detection algorithm.

B. EEG signal decomposition

As demonstrated in

Figure 2, in EEG the composite signal of one electrode is a summation of four (not considering the gamma wave) individual brain waves and some added noise. The individual brain waves are identified by their frequencies. To analyze each brain wave individually, 4 band pass filters (Chebyshev type II of 18^{th} order) were applied to the signal (in frequency domain), to decompose the original signal into the 4 desires brain waves (Delta, Alpha, Theta and Beta).
With the brain wave frequency bands being so close to each other and with small frequencies, a threshold of 0.5 Hz was considered when applying the minimum and maximum values of cutoff frequency (represented in Figure 7). The added interval to the domain of the frequency for each brain wave, will be partially discarded in the transition phase. This ensures the least data loss for each brain wave.

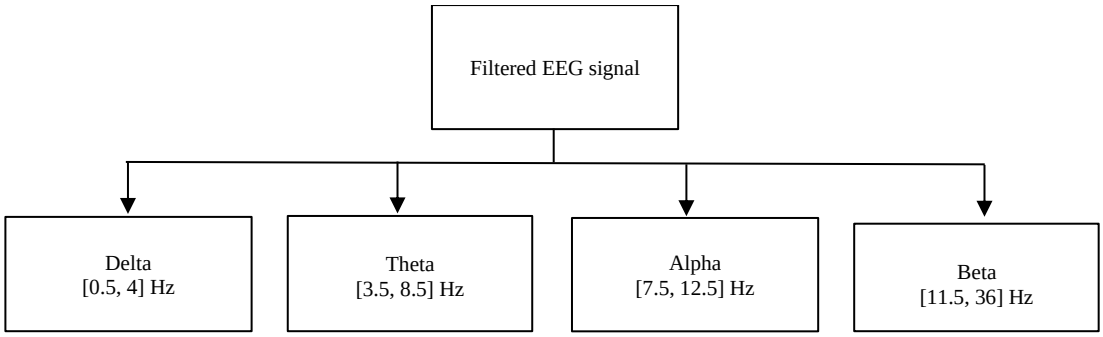

Figure 7. Visual representation of the algorithm and cutoff frequencies used to decompose the EEG signal.

C. Spike detection

To detect CAE representing spikes, cross correlation function was used. This function is a part of signal package in octave. As mentioned earlier, delta waves are the sub waves that most strongly express epileptic activity. Hence, delta is the brain wave used for the spike detection.

The cross-correlation function was applied to the signal in the time domain, therefore, initially an inverse FFT (IFFT) was applied to the signal. Changing back to the time domain, the zeros added by FFT had to be removed, to mimic the initial signal. To take the zeros a function was implemented where values smaller than a certain number are passed to zero and a while loop is used to remove the indices, if the average of the next 200 values is equal to zero.

The spike samples used in the correlation function were extracted manually from EEG signals with epileptic activity.

One of the returned variables of the cross-correlation function is an array of numbers, which represents the correlation of each point of the EEG signal with the sample segment (R). This value was used to define thresholds and detect epileptic activity. This was achieved by a normalization factor, being the average value of R, divided by the maximum value of R, applied in a sliding window. This way, the results are provided for the examiner are marked with an alert, in windows where discharge is detected.

5 Results and Discussion

A Chebyshev type II filter of 18^{th} order, with ripple of 50 that was applied to the EEG signal. After trying and observing every type of filters applied to the EEG, the Chebyshev type II was the filter that presented better results in the filtered signal. This order was chosen because of the steep transition phase it provides. The generation and application of the signal takes an average of 1.5 microseconds. This order was also examined with the 2^{nd} order, and the execution time was dropped to 0.38 microseconds. Regardless of the difference in execution time, the 18^{th} order filter was still very fast, and the results were much more promising.

The result of the EEG decomposition that were done according to Figure 7 (Alpha, Beta, Theta and Delta wavelets) are presented in Figure 8. Because of the transition phase of the filter, the cutoff frequencies for brain waves were given a margin, to avoid loss of relevant data. As visible in Figure 8, there is a small gap between alpha and beta waves, which is due to the same fact. But, because we are only considering the delta wave in this work, this detail it’s not relevant.

After the IFFT is applied to the delta brain wave and the unwanted zeros are removed, spike detection algorithm is applied (cross correlation function). With the values obtained from this function, a thresholding is done, and final results are presented.

Due to the lack of resources (including low CPU power of computers), and short amount of time for this project the authors could only achieve part of the desired objectives. It is proven that the code is functional as it detects epilepsy only for positive cases.

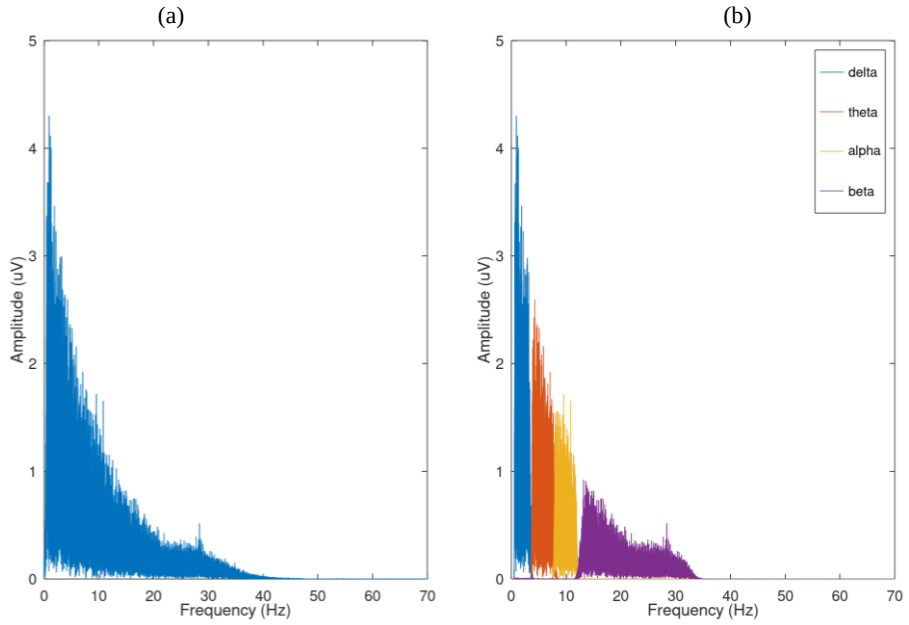

Figure 8. (a) EEG signal in frequency domain (after noise removal) (b) Decomposed EEG signal to 4 brain waves (Graphs generated in GNU Octave).

5.1 Detection accuracy

As mentioned in table 4 epilepsy samples and 1 control EEG signals were tested with the algorithm. Out of 4 EEG datasets, all CAE cases were detected, and as expected, for the control case epileptic discharge was not detected.

6 Conclusion

The proposed algorithm offers an efficient automatic detection scheme that can be used in diagnostic and therapeutic evaluations in patients with absence seizures.
The processing of the data was done in the frequency domain, but the detection was done in the time domain. Various alteration of the domain can affect the signal. The discharges would ideally be detected in the frequency domain.
The FFT function was applied with a bigger size than the original signal, creating a series of zeros in the beginning of the signal. The number of these zeros depends on the size of the original signal but can occupy up to nearly half of the result (after application of FFT and iFFT). This could be avoided by instead of using an FFT dependent on the length of EEG signal, using an FFT with a smaller size, and applying it with a sliding window throughout the whole signal.
The proposed method detected CAE in all databases with this diagnosis. The time of execution for the algorithm is 250 seconds (for an EEG file with XX samples and a computer with Intel Core i5 CPU), taking most of the time to upload the EEG file. In a real time, analysis, the algorithm is expected to take much less time. When artifacts are present in the control (healthy) EEG, false detection rate increases, which decreases the specificity of the algorithm. To avoid this false positive diagnosis, a deeper cleaning must be applied to the signal at the pre-processing phase. A total of 5 EEG signals was tested, with 4 of them being diagnosed with CAE in this work. The processing is never going to be perfect, especially because of the interaction of muscle activity artefact with EEG signal, which can lie in the same frequency interval.

In future works, the study should be tested with a wider variety of EEG samples of cases of CAE, as well as control, to confirm the viability of this method. As an upgrade, a higher number of spike waves should be added to our dataset of SWD, with variety in durations and amplitude. This will increase the accuracy of the results obtained from the cross-correlation function, leading to a more exact diagnosis. Research and more development should be applied to extend this technique on a continuous EEG database and for a greater number of subjects.

It is known that CAE seizures are often set off by a period of hyperventilation. In future studies, EEG samples can be tested along with a pneumogram, to make sure the SWD being detected is most probably from a CAE seizure, and not caused in the EEG by muscle or environment artefacts. Ideally a graphical representation of the results would be provided for non-tech savvies, with specificity of the intensity of the CAE. Several methods were tested to achieve this, but unfortunately out tries were unsuccessful.

7 Acknowledgment

The authors would like to thank Neuroimprove clinic for providing the EEG signal datas, as well as the reports of their evaluations. We would also like to thank our supervisor, professor Joaquim Alves, for helping us throughout this project.

8 References

II. BIBLIOGRAPHY

A. Pavone, E. N. (2000). Absence seizures and the frontal lobe. *PubMed*.

Abhang, P. A., Gawali, B. W., & Mehrotra, S. C. (2016). Chapter 3 - Technical Aspects of Brain Rhythms and Speech Parameters. In P. A. Abhang, B. W. Gawali, & S. C. Mehrotra. (Eds.), *Introduction to EEG- and Speech-Based Emotion Recognition.* Academic Press. doi:https://doi.org/10.1016/B978-0-12-804490-2.00003-8.

Albuja, A. C., & Khan., G. Q. (2021, 12 13). *Absence Seizure*. Retrieved from StatPearls Publishing: https://www.ncbi.nlm.nih.gov/books/NBK499867/

APTECH. (n.d.). *Permutation Entropy - Aptech*. Retrieved from https://www.aptech.com/blog/permutation-entropy/

Asanagi. (2022). *Ficheiro:21 electrodes of International 10-20 system for EEG.svg*. Retrieved from https://pt.m.wikipedia.org/wiki/Ficheiro:21_electrodes_of_International_10-20_system_for_EEG.svg

Aslani, S. (2022). Retrieved from Neuroimprove Clinic: https://neuroimprove.pt

Berman, R., Negishi, M., Vestal, M., & Spann, M. (2010). *Simultaneous EEG, fMRI, and behavior in typical childhoodabsence seizures.*

Dan, J., Vandendriessche, B., Paesschen, W. V., Weckhuysen, D., & Bertrand, A. (2020). Computationally-Efficient Algorithm for Real-Time Absence Seizure Detection in Wearable Electroencephalography. *International Journal of Neural Systems*. doi:https://doi.org/10.1142/S0129065720500355

Frontiers, N. (n.d.). *New Frontiers Psychiatry*. Retrieved from https://www.newfrontierspsychiatry.com/why-is-the-dorsolatereral-prefrontal-cortex-dlpfc-the-favorite-region-to-stimulate/

FS, T., & JR, K. (1989). Fundamentals of EEG Technology. *Basic Concepts and Methods, 1*.

Glaba, P., Latka, M., & West, B. J. (2021). Absence Seizure Detection Algorithm for Portable EEG Devices. *Frontiers in Neurology , 12*. doi:https://doi.org/10.3389/fneur.2021.685814

Hao, Y., Khoo, H. M., Ellenrieder, N., Zazubovits, N., & Gotman, J. (2018). DeepIED: An epileptic discharge detector for EEG-fMRI based on deep learning. *NeuroImage: Clinical, 17*, 962-975. doi:https://doi.org/10.1016/j.nicl.2017.12.005

HL, A., & WA, M. (1989). *Essentials of Neurophysiology.* Canada.

Homan, R., Herman, J., & Purdy, P. (1987). Cerebral location of international 10–20 system electrode placement. *Electroencephalography and Clinical Neurophysiology, 66*(4), 376-382.

Jasper, H. (1958). The Ten-Twenty Electrode System of the International Federation. *Electroencephalography and Clinical Neurophysiology, 10*, 371-375.

Johns Hopkins Medicine. (n.d.). *Absence Seizures | John Hopkins Medicine*. Retrieved from Absence Seizures: https://www.hopkinsmedicine.org/health/conditions-and-diseases/epilepsy/absence-seizures

Jon-Paul A. Manning, D. A. (2003). Pharmacology of absence epilepsy. *TRENDS in Pharmacological Sciences*.

M.D., N. E. (2006). Absence Seizures. In N. E. M.D., *Current Therapy in Neurologic Disease (Seventh Edition).*

Maingard, J. B. (n.d.). *D. Frontal lobe.* Retrieved from Radiopaedia: https://doi.org/10.53347/rID-25358

Malik, A. S., & Ullah Amin, H. (2017). Chapter 1 - Designing an EEG Experiment. In A. S. Malik, & H. Ullah Amin (Eds.), *Designing EEG Experiments for Studying the Brain* (pp. 1-30). Academic Press. doi:https://doi.org/10.1016/B978-0-12-811140-6.00001-1

Medical News Today. (n.d.). *Four types of Epilepsy, their symptoms and treatments*. Retrieved may 21, 2022, from https://www.medicalnewstoday.com/articles/types-of-epilepsy#diagnosis

Nadia Mammone, J. D.-H. (2015, july 2). Differentiating Interictal and Ictal States in Childhood Absence Epilepsy through Permutation Rényi Entropy. *MDPI*.

NHS. (n.d.). *Epilepsy - NHS*. Retrieved may 20, 2022, from https://www.nhs.uk/conditions/epilepsy/

Niedermeyer, E., & Lopes da Silva, F. (1993). *Electroencephalography: Basic Principles, Clinical Applications and Related Fields* (3 ed.). Philadelphia: Lippincott, Williams & Wilkins.

NTI Audio. (2022). Retrieved from https://www.nti-audio.com/en/support/know-how/fast-fourier-transform-fft

Robert S. Fisher, H. E. (2015, march 27). How Can We Identify Ictal and Interictal Abnormal Activity? *National Library of Medicine*.

Rochelle Caplan, J. L. (n.d.). Frontal and temporal volumes in ChildhoodAbsence Epilepsy. *Eplilepsia*, 7.

Rojas, G., & Galvez, M. (2018). Study of Resting-State Functional Connectivity Networks Using EEG Electrodes Position As Seed. *Frontiers in Neuroscience*.

Sara Matricardi MD, A. V. (2014). Current Advances in Childhood Absence Epilepsy. *Pediatric Neurology*, 8.

Segan, S. (2018, Sep). *Absence Seizures*. Retrieved 04 04, 2022, from Medscape: https://reference.medscape.com/article/1183858-overview

Siuly, S., Li, Y., & Zhang, Y. (2016). Electroencephalogram (EEG) and Its Background. *EEG Signal Analysis and Classification. Health Information Science*. doi:https://doi.org/10.1007/978-3-319-47653-7_1

Taeho Kim, P. N. (2020, July 21). Epileptic Seizure Detection and Experimental Treatment: A review . *frontiers in Neurology*, p. 24.

Tuncera, E., & Bolat, E. D. (2022). Channel based epilepsy seizure type detection from electroencephalography (EEG) signals with machine learning techniques. *Biocybernetics and Biomedical Engineering, 42*(2), 575-595.

Xanthopoulos, P., Rebennack, S., Liu, C.-C., & Zhang, J. (2010). A novel wavelet based algorithm for spike and wave detection in absence epilepsy. *10th IEEE Int. Conf. Bioinformatics and Bioengineering*, 14–19.

9 Appendix

A. Appendix I. Generation of electrical fields in brain.

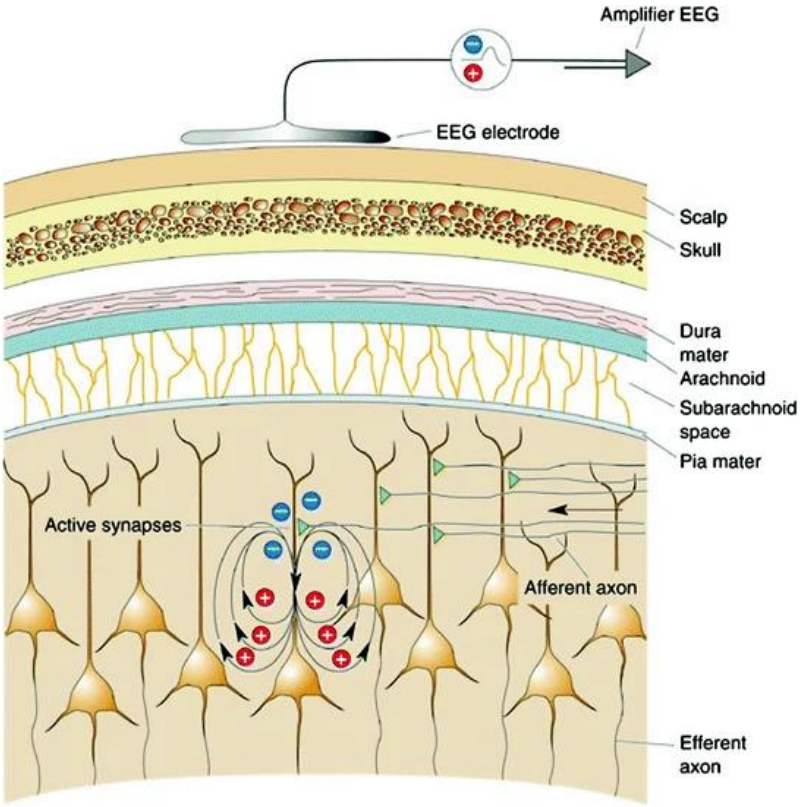

Figure 9. Illustration of generation of very small electrical fields by synaptic currents in pyramidal cells. The EEG electrode measures the signal through the thick layers of tissues. Only if thousands of cells simultaneously their small voltages can the signal become large enough to be seen at the surface of the scalp (Ref. (Siuly, Li, & Zhang, 2016)).

B. Appendix II. 10-20 electrode positioning system.

The International Federation of Clinical Neurophysiology (http://www.ifcn.info) adopted the standardization for EEG electrode placement called 10–20 electrode placement protocol (Jasper, 1958). A basic assumption in this process is that there is a constant correlation between these scalp locations and underlying cerebral structures.

This system of electrode placement employs measurements of external cranial landmarks to locate electrodes on the scalp. It standardized the physical placements and designations

of 21 electrodes on the scalp. Using reference points on the skull in the nasion, preauricular points and inion, the head is divided into proportional positions to provide adequate coverage of all the brain regions. The name of each electrode consists of a letter and a number. The letter refers to the region of the brain where the electrode is positioned (F: frontal, C: central, T: temporal, P: posterior, and O: occipital), and the number is related to the cerebral hemisphere (even numbers in the right hemisphere, and odd numbers in the left; Figure 10) (Rojas & Galvez, 2018; Homan, Herman, & Purdy, 1987).

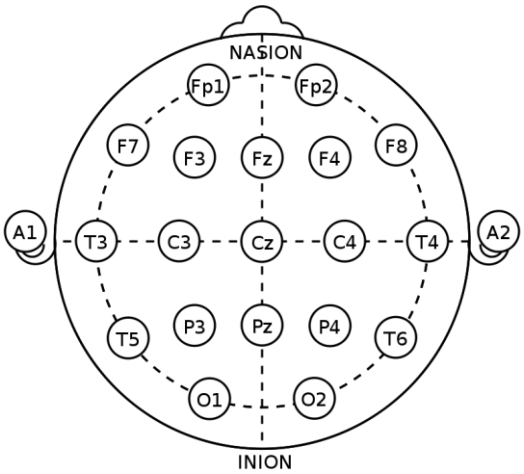

Figure 10. The 10-20 International system of EEG electrode placement (ref. (Asanagi, 2022))